

Integral space–time scales in turbulent wall flows

Maurizio Quadrio^{a)}

Dipartimento di Ingegneria Aerospaziale del Politecnico di Milano, via La Masa 34, 20156 Milano, Italy

Paolo Luchini^{b)}

Dipartimento di Ingegneria Meccanica dell'Università di Salerno, 84084 Fisciano (SA), Italy

(Received 19 December 2002; accepted 2 May 2003; published 25 June 2003)

A direct numerical simulation of the Navier–Stokes equations is used to compute the space–time correlations of velocity fluctuations in a turbulent channel flow. By examining the autocorrelation $R(\xi, \tau)$ of the longitudinal wall shear-stress as a function of the streamwise and temporal separations, the effects of the limited extent of the computational domain when (artificial) periodic boundary conditions are used can be described and quantified. A time scale similar to the conventional integral scale but statistically related to the life time of the turbulent structures is computed from spatio-temporal data. The convection velocity, defined as the direction in the ξ, τ plane where the autocorrelations have their maximum at vanishingly small time delay, is computed as a function of the distance from the wall, and compared with the data available in the literature. Based on autocorrelations, the accuracy within which Taylor's hypothesis is verified is quantitatively assessed. Last, the effect of the spatial discretization on the statistical characterization of wall turbulence is discussed. © 2003 American Institute of Physics. [DOI: 10.1063/1.1586273]

I. INTRODUCTION

Many research papers of the last decades have described the complex scenario of a turbulent flow over a wall as a distribution of coherent turbulent structures superimposed on to a random background. The intrinsic stochastic character of such a scenario has not prevented us from understanding that some structures are of greater temporal coherence than others, and travel for a relatively long time interval in the direction of the mean flow during their lifetime. In certain cases, only the observation of the flow in a Lagrangian reference frame brought out that some structures, while appearing highly fluctuating when observed in a Eulerian reference frame, remain however coherent for a relatively long time when followed during their evolution. For example, Johansson *et al.*¹ discovered that, although the spatial structure of high- $u'v'$ regions is spotty, each spot can be traced along in its motion for more than 100 viscous time units. (Here and in the following a prime denotes fluctuating values around space–time averages; u , v , and w are the velocity components in the streamwise x , wall-normal y and spanwise z directions, respectively.) A similar conclusion was arrived at by Kim and Hussain² for the relatively short, quasi-streamwise near-wall vortices, which are temporally persistent structures and lead the low-speed streaks, typical of the near-wall region of turbulent flows.

It becomes then natural to distinguish between a spatial length scale typical of a structure at fixed time (its “length,” as deduced, for example, from a snapshot of the flow field) and another, unrelated, spatial scale corresponding to the distance traveled in the mean flow direction by the structure

during its entire lifetime. A similar distinction can be made for time scales: They can indeed be related to space scales by the notion of convection velocity and by Taylor's frozen-turbulence hypothesis,³ so often invoked by experimentalists when converting time-dependent data into measurements depending on the streamwise coordinate. A number of early experiments (see for example Favre *et al.*^{4,5}) were aimed at the evaluation of the convection velocity C in turbulent wall flows, showing that in the outer region of a boundary layer or channel flow C is very near to (slightly less than) the local mean velocity. This otherwise reasonable result was implicitly extended to the near-wall region, and the convection velocity has been since then often thought of as strictly related to the local mean velocity of the flow. In an experimental work based on the analysis of frequency-wavenumber velocity spectra,⁶ Morrison, Bullock, and Kronauer obtained a first estimate of the value of C in the near-wall region. Kreplin and Eckelmann⁷ were able to measure the two components of wall friction and two velocity components at several distances from the wall in an oil channel at low Reynolds number; the correlation functions computed from these measurements highlighted the convective nature of the flow in the viscous sublayer, and space–time features of the statistically dominant near-wall turbulent structures were proposed.

In more recent years, mainly thanks to the analysis of a database produced by Kim *et al.*⁸ through direct numerical simulation (DNS) of a plane channel flow governed by the incompressible Navier–Stokes equations, a more detailed comprehension of the advection process of flow structures in the near-wall region has become possible. Piomelli *et al.*⁹ supported the validity of Taylor's hypothesis in the buffer layer and above. Johansson *et al.*¹ traced in time the streamwise evolution of turbulent structures deduced via a conditional-sampling technique, and visually estimated a

^{a)}Electronic address: maurizio.quadrio@polimi.it

^{b)}Electronic address: luchini@unisa.it

convection velocity for such structures of $10.6 \pm 1 u_\tau$ (u_τ being the friction velocity). Choi and Moin¹⁰ and Jeon *et al.*¹¹ computed convection velocities of pressure and shear fluctuations at the wall, and Kim and Hussain² first discovered and emphasized the important difference between the local mean velocity and the convection velocity in the near-wall region. The effect of the turbulent structures present in the buffer layer and beyond is such that their “footprints” are felt all the way down to the wall: a convection velocity of flow perturbations is well defined even at the wall, where the local velocity is zero, and remains approximately constant in the viscous sublayer, with a value of the order of the mean velocity at $y^+ = 15$ (quantities shown with a + superscript are made dimensionless with the friction velocity and the kinematic viscosity of the fluid). On the experimental side, a renewed interest is evident in the recent papers by Krogstad *et al.*¹² and by Khoo *et al.*,¹³ who were able to accurately measure the streamwise component of velocity, in low- and medium-Reynolds-number turbulent flows, down to 2 wall units from a solid wall, and to obtain estimates of \mathcal{C} based on two-point correlations. It must be said, however, that subsequent experimental measurements of \mathcal{C} by Khoo *et al.*¹⁴ disagree with DNS data, which on their side have been computed in several papers but always using the same database, as explicitly noted by Khoo *et al.*¹⁴ An independent confirmation of these results can, therefore, be useful. Moreover, the effect of the main computational parameters on the DNS-computed values of \mathcal{C} has not been addressed yet; in particular the effect of the periodic-box size and of the time step on \mathcal{C} is unknown.

Coming back to space- and length-scales, the average lifetime of the near-wall turbulent structures often remains inaccessible to experimental measurement, even when Taylor’s hypothesis is employed, owing to the difficulty of simultaneously acquiring time- and space-dependent measurements, whereas it can be evaluated numerically through a DNS with relative ease. In such computations, however, the unbounded space in the homogeneous directions is replaced by a periodic computational domain of finite length and width. The consequence is that a third, artificial space (and hence time) scale enters the picture. Only if the instantaneous dimensions of the structures and their lifetime can be verified to be independent of this artificial periodicity will they possess physical meaning.

In the current DNS literature, the adequacy of the longitudinal period of the computational box is usually ascertained, following Kim *et al.*,⁸ by verifying that the two-point correlation function for some fluid variable (notably the u component of velocity, which is known to possess the widest space scales) at some distance from the wall becomes sufficiently small at a streamwise separation ξ equal to half the box length, while zero time and spanwise separation is implicitly assumed. This amounts to considering a snapshot of turbulent structures at any given time, ensuring that the box is long enough to contain the longest of them. On the other hand, the question of whether the full lifespan of the structure can be followed reliably in the computations still has to be rigorously addressed. Just a few papers have computed some space–time correlations for turbulent wall flows from

DNS. For example, Choi and Moin¹⁰ computed information on the space–time characteristics of wall-pressure fluctuations in a channel flow, and Jeon *et al.*¹¹ extended the same analysis to wall shear-stress fluctuations, but they did not use their results to assess the adequacy of the space–time truncated computational domain. The recent paper by Phillips¹⁵ investigates in some theoretical detail the behavior of space–time correlation functions, and uses the DNS data by Kim and Hussain² as a test case.

In this paper we use space–time velocity, wall-pressure and wall-shear spectra, computed through a purposely executed DNS of turbulent plane channel flow, to investigate to what extent the longest temporal scales of wall turbulence are affected by the size of the computational box. We moreover compute a time scale related to the average life of turbulent structures. We then introduce a correlation-based definition of convection velocity \mathcal{C} , through which the validity of Taylor’s hypothesis and the sensitivity of \mathcal{C} to the main computational parameters are examined. In particular the error associated with the use of Taylor’s hypothesis can be precisely quantified.

II. NUMERICAL PROCEDURES

For this work we used a computer code, recently developed by Quadrio and Luchini,¹⁶ which is a pseudo-spectral solver of the incompressible Navier–Stokes equations written, similarly to Kim *et al.*,⁸ in terms of a scalar equation for the wall-normal component of vorticity and a scalar equation for the normal component of velocity, in a way that imitates the Squire decomposition of stability problems. Fourier expansions are applied in the homogeneous directions, whereas compact fourth-order finite differences are used in the wall-normal direction, acting on a five-point computational stencil in a variable-spacing mesh. The code is parallel, can take advantage of both SMP shared-memory architectures and distributed-memory networked computers; it presently runs on a low-cost fully dedicated system composed of 8 SMP commodity personal computers with two Pentium III 733 MHz CPUs each. The simulations are performed at a Reynolds number $Re_\tau \approx 180$, based on the friction velocity and h , half the channel height. The size of the periodic computational box (except where explicitly changed to verify its effects) is $L_x = 4\pi h$ (2253 viscous lengths) and $L_z = \frac{4}{3}\pi h$: this corresponds to the typical box dimensions that are usually considered acceptable at this value of Re in the current literature.¹⁷ The spatial discretization also takes on currently accepted sizes:¹⁷ The wall-normal direction is discretized with 129 mesh points, 193 streamwise and 129 spanwise Fourier modes are used in the homogeneous directions. The equivalent spatial resolution is $\Delta x^+ = 11.7$, $\Delta z^+ = 5.9$, and $\Delta y^+ = 0.8$ – 4.7 from the wall to the channel centerline. Dealiasing is performed by expanding the number of collocation points by a factor (at least) $3/2$ before going from Fourier space into physical space and contracting on the way back. The equations are integrated in time following the commonly used partially implicit approach, with a third-order Runge–Kutta scheme for the convective terms and a second-order Crank–Nicholson scheme for the implicit

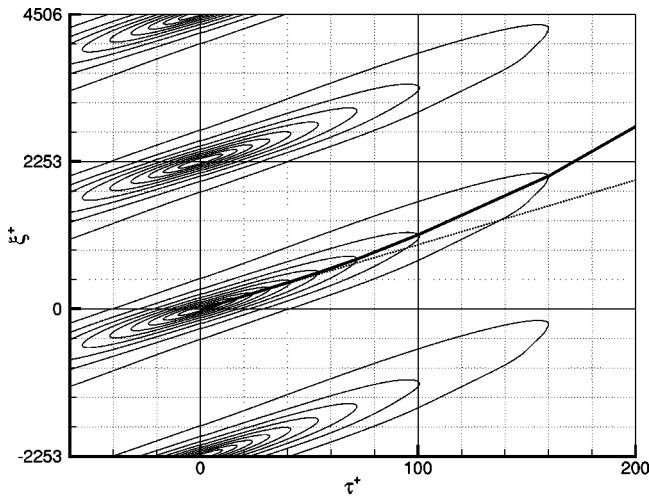


FIG. 1. Autocorrelation function $R(\xi^+, \tau^+)$ for the longitudinal shear-stress at the wall. Isolines are from 0.1 to 0.9 by 0.1. The thick line connects fixed-time spatial maxima of R ; the dotted straight line is drawn along the direction of maximum correlation at the origin.

terms. The time step is 0.075 viscous time units, and all the simulations have been run for a time interval of 4500 viscous time units.

Space-time correlations are computed after writing to disk, every 1.5 viscous time units for the full duration of the simulation, the Fourier coefficients of the flow variables at the wall (namely pressure and the two components of the shear stress), and the coefficients of the three velocity components at the distance from the wall of $y^+ \approx 10$. The autocorrelation function $R(\xi, \tau)$ for each flow variable is computed directly in the physical domain as far as its time dependence is concerned, whereas the dependence on the spatial separation ξ is obtained from the inverse Fourier transform of the spectral density function $S(\alpha, \tau)$, where α is the streamwise wavenumber. All correlation data shown below refer to a null separation in the spanwise direction.

III. SPACE-TIME CORRELATIONS

Reported in Fig. 1 is the autocorrelation function $R(\xi, \tau)$ for the x component of the wall shear-stress. The temporal and spatial separations are expressed in viscous units; the spatial separation spans three times the channel length, which amounts to 2253 wall units. The maximum temporal separation considered is from $\tau^+ = -380$ to $\tau^+ = 380$, even if a shorter time scale is shown on the plot, namely from $\tau^+ = -60$ to $\tau^+ = 200$.

The periodicity of the flow in the longitudinal direction is reflected in the appearance of repeated images, whose longitudinal separation is exactly one channel length. The mean velocity at the wall is zero, but nonetheless the convective nature of the flow at the wall is clearly indicated by the elongated shape of the autocorrelation contours: a preferred direction in the ξ, τ plane is indeed associated to a characteristic velocity. This direction, evaluated at the origin, is indicated with a dotted line. In Fig. 1 a thick line is drawn connecting fixed-time spatial maxima of the autocorrelation function; its significance will be illustrated in the next Section.

This plot is qualitatively similar to the analogous figure by Jeon *et al.*¹¹ The most significant quantitative difference is the extent of the low-correlation region: the present results indicate that the correlation remains above 0.1 for values of τ^+ up to 160, contrary to their indication of $\tau^+ = 90-100$. As a possible explanation of this discrepancy we might surmise that their window function, employed when converting temporal data into frequency data and back in the process of obtaining correlations, could have affected the correlations at large time separation. It must also be observed that they averaged over relatively few time histories, and were somehow limited by the adopted discretization: The total averaging time was 907.2 viscous time units, further subdivided in six overlapping subintervals (with 50% overlap), so that the maximum considered time delay was only $\tau^+ = 129.6$.

The autocorrelation functions for the other flow variables at the wall, namely the spanwise component of the wall

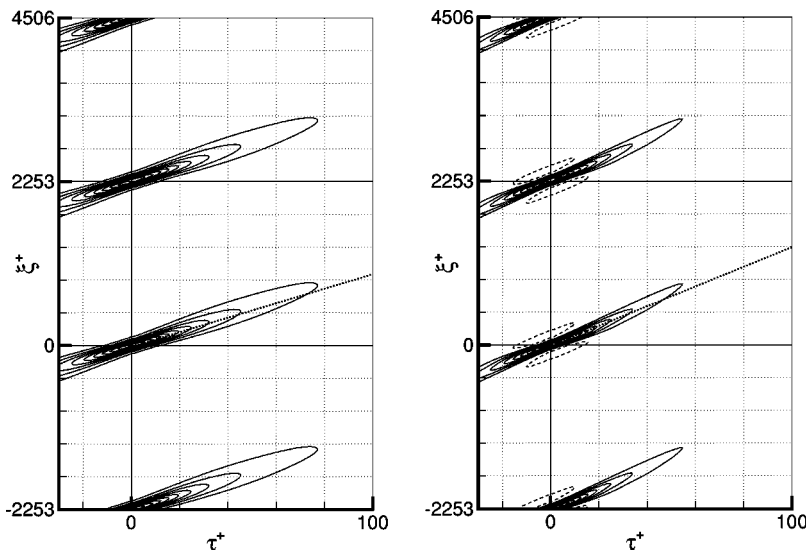


FIG. 2. Autocorrelation function $R(\xi^+, \tau^+)$ for the spanwise shear-stress (left) and pressure (right) at the wall. Isolines are from 0.1 to 0.9 by 0.1; dashed contours are for the level -0.05 . The dotted straight lines are drawn along the direction of maximum correlation at the origin.

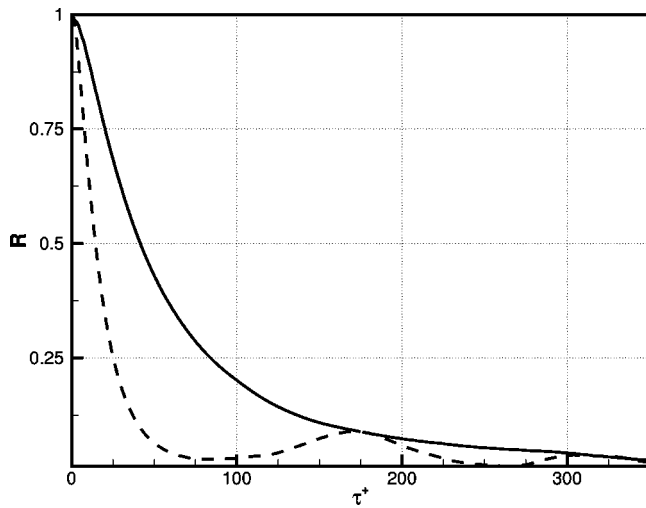


FIG. 3. Time correlation of the longitudinal shear-stress at the wall for zero streamwise separation (dashed line) and along the line of correlation maxima (continuous line).

shear-stress and the pressure, are shown in Fig. 2. These flow quantities show significantly shorter characteristic length and time scales, which might also explain why they are in much better quantitative agreement with Jeon *et al.* results. A small region of negative correlation for p can be noted at small time delays (or small streamwise separations). A similar slope of the line of autocorrelation maxima is observed for spanwise as for streamwise shear, but for pressure this slope is significantly higher, suggesting a larger propagation velocity of pressure fluctuations near the wall.

IV. INTEGRAL TIME SCALE

A common quantitative characterization of the time needed for a signal to decorrelate is the so called integral scale; in the real, nonperiodic, flow the integral scale can be computed from the space–time correlation function evaluated at $\xi=0$, as

$$T = \int_0^{\infty} R(0, \tau) \, d\tau. \quad (1)$$

In Fig. 3 the quantity $R(0, \tau^+)$ is reported with a dashed line for the x component of the wall shear-stress. It exhibits a first minimum at a temporal separation of $\tau^+ \approx 85$, followed by a secondary peak at $\tau^+ \approx 170$; a third peak at $\tau^+ \approx 320$ is also discernible. This sequence of peaks is an artifact due to repeated passage of the same structures, advected through the computational box of finite length: Owing to the periodic boundary conditions, the structures that leave the computational domain from the downstream side re-enter from the upstream side, thus producing a peak in the time correlations.

The integral scale T (expressed in viscous units) would be the area under the dashed line of Fig. 3, if it were not for the aliased images of the correlation peak. A simple but accurate way to account for the aliasing effect is to truncate the integral at the first minimum of the curve. In fact, this amounts to an exponential fitting of the tail of the autocorre-

TABLE I. Integral time scale T and life-time scale T^ℓ for the components of velocity at the wall and at $y^+ \approx 10$. All values are in viscous time units.

	$y^+ \rightarrow 0$	$y^+ \approx 10$
T_u	19.1	19.2
T_u^ℓ	61	68
T_v	...	6.5
T_v^ℓ	20	23
T_w	6.1	7.0
T_w^ℓ	30	46
T_p	2.3	...
T_p^ℓ	22	...

lation function: It can be shown that, if the tail were exponential, the missing part of the integral from the truncation point up to infinity would be exactly made up for by the tail of the second peak protruding into the first.

The integral scale of turbulence in homogeneous isotropic flows has received much experimental and numerical attention,^{18,19} but values of T for wall-bounded turbulent flows computed from a DNS are not to date known. Khoo *et al.*¹⁴ experimentally measured for the u velocity component in the very near-wall region of a turbulent channel flow a value of $T_u^+ \approx 15$; for comparison, not having found any suitable previous experimental measurements, they indirectly estimated $T_u^+ \approx 20$ from numerical data: Namely as the ratio between the integral longitudinal space scale, computed from the spatial autocorrelation function $R(\xi, 0)$ at $y^+ = 5.4$ obtained in the DNS of Kim *et al.*,⁸ and the near-wall convection velocity C_u , as determined by Kim and Hussain.² Our own result obtained from integrating $R(0, \tau^+)$ down to its first minimum, probably the first computation of T at the wall from DNS data, is an integral time scale $T^+ = 19.1$ for the streamwise shear-stress at the wall. Furthermore, the integral time scale is 6.1 viscous time units for the spanwise shear, and 2.3 for the pressure; at $y^+ \approx 10$ the time scales for the u , v and w velocity components become 19.2, 6.5, and 7.0, respectively. These results are summarized in Table I, together with the alternative time scale discussed in the following.

Integral life scale

Another interesting integral time scale, with a completely different physical meaning, can be introduced to quantify the life time of the turbulent structures. This integral life scale, which will be denoted as T^ℓ in the following, can be computed through the integration of $R(\xi^+, \tau^+)$ along the path of maximum correlation, i.e., along the thick solid line drawn in Fig. 1 and connecting fixed-time spatial maxima of the autocorrelations. The integrand function, for the streamwise shear, is shown as a solid line in Fig. 3 compared with the integrand in the definition of the conventional integral scale. While the integral scale T defined by Eq. (1), from a physical viewpoint, is related to the local visibility of the turbulent structures at a given location in space, the scale T^ℓ relates to the complete life cycle of turbulent structures, since it quantifies how long the signal takes to decorrelate when followed in its motion. The present data give T^ℓ equal to 61

viscous time units for the longitudinal shear, 30 for the spanwise shear and 22 for the pressure fluctuations at the wall. At $y^+ = 10$ the lifetimes become $T_u^\ell = 68$, $T_v^\ell = 23$, and $T_w^\ell = 46$ viscous time units. One can note the interesting fact that pressure structures are characterized by the smallest temporal scales when observed in a Eulerian frame ($T_p = 2.3$), but their size becomes comparable to the others when considered in a Lagrangian frame ($T_p^\ell = 22$). Time scales tend moreover to increase slightly with increasing distance from the wall.

V. CONVECTION VELOCITY

A convection velocity \mathcal{C} , with which perturbations are on average convected, can be preliminary estimated from the repeated peaks of the correlation function reported in Fig. 3, as the ratio of the box length and the time delay at which the first peak is observed. It is immediately evident that the typical convective time taken by the structures to turn around a computational box of this size is shorter than their typical life cycle.

More precisely identified definitions for the convection velocity are based on local slopes of either autocorrelation functions or spectral density functions.^{2,10,11} Spectrum-based definitions, however, suffer from the inherent statistical error associated with the estimation of the spectrum from a finite sample, which does not decrease with increasing sample size unless an artificial windowing is introduced. A correlation-based definition, on the other hand, has an estimation error that decreases with the square root of the number of samples.²⁰ Hence in the present work we define a convection velocity based on the analysis of autocorrelation functions, as the ratio ξ/τ where $R(\xi, \tau)$ is a maximum, for a given time delay. The thus obtained velocity only slightly changes when different temporal separations are considered, in the range where the correlation function remains significantly different from zero, as evident from our Fig. 1 and from Kim and Hussain.² The mild increase with increasing separation can be related to a tendency of large structures to be advected faster than small structures.

In their own work on the convection velocity, Kim and Hussain² searched for the maximum of the correlation function at a fixed time delay using a pre-computed spatial grid. They reasoned that when the time delay is too large there is a significant statistical error in estimating the correlation function, whereas when τ is too small an error is produced by the interpolation between adjacent ξ -grid points. A balance between these two error sources led them to choose as a compromise the particular value of $\tau^+ = 18$. Here we do not have the second type of error because we directly compute the correlation function from its spectral components without any grid interpolation, and thus can work with infinitesimal τ without any difficulty.

Hence we define \mathcal{C} at vanishingly small time delay, i.e., as the slope of the dotted straight line through the origin shown in Figs. 1 and 2, namely

$$\mathcal{C} = - \left. \frac{\partial^2 R / \partial \xi \partial \tau}{\partial^2 R / \partial \xi^2} \right|_{\xi, \tau=0}.$$

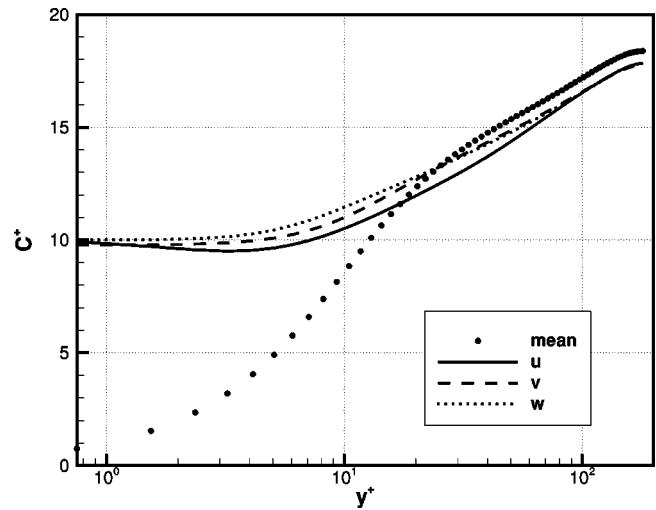


FIG. 4. Propagation velocity for the three velocity components across the channel, compared to the mean velocity profile.

Computationally the easiest way to obtain this value is to use the time delay corresponding to one time step Δt of the calculation, by looking for the value of ξ where

$$\frac{\partial}{\partial \xi} R(\xi, \Delta t) = 0.$$

The corresponding \mathcal{C} is computed in Fourier space by a Newton iteration, which leads to the formula

$$\mathcal{C}^{n+1} = \mathcal{C}^n + \frac{\sum_{\alpha} S(\alpha, \Delta t) i \alpha \exp(i \alpha \mathcal{C}^n \Delta t)}{\Delta t \sum_{\alpha} S(\alpha, \Delta t) (i \alpha)^2 \exp(i \alpha \mathcal{C}^n \Delta t)},$$

where n is the iteration level, and $S(\alpha, \Delta t)$ is obtained, independently of n , by time-averaging products of corresponding velocity Fourier components at a given distance from the wall and a time separation of $\tau = \Delta t$. Convergence is achieved in just two or three iterations.

Figure 4 reports the variation of \mathcal{C} with distance from the wall (in viscous units) for the three velocity components, and Table II shows the numerical values at the wall and at $y^+ \approx 10$. There is a general agreement with previously reported propagation velocities computed from older numerical databases, which are thus now independently confirmed. Some small differences can, however, be noticed in comparison to Kim and Hussain.² In particular our \mathcal{C}_u^+ profile for the u velocity component exhibits a nonmonotonic behavior, with a minimum of 9.5 at $y^+ = 3.2$. On the other hand, the wall values of $\mathcal{C}_u^+ = 9.93$, $\mathcal{C}_v^+ = 9.79$ and $\mathcal{C}_w^+ = 10.01$ are in very good agreement with those by Kim and Hussain, and do not appreciably change when the \mathcal{C} 's are computed, like their own, at $\tau^+ = 18$ (e.g., $\mathcal{C}_u^+ = 9.91$). Experimental measure-

TABLE II. Convection velocity for the components of velocity fluctuations at the wall and at $y^+ \approx 10$.

	$y^+ \rightarrow 0$	$y^+ \approx 10$
\mathcal{C}_u^+	9.93	10.38
\mathcal{C}_v^+	9.79	10.85
\mathcal{C}_w^+	10.01	11.32

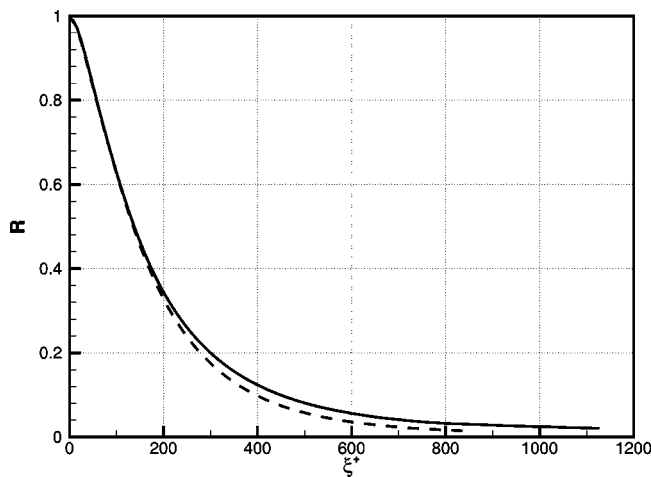


FIG. 5. Verification of Taylor's hypothesis: Spatial correlation at zero time delay for the longitudinal wall-shear (continuous line) and temporal correlation plotted against the abscissa $C_u^+ \tau^+$ with C_u^+ evaluated at the wall (dashed line). Periodicity effects have been compensated for through an exponential fitting.

ments by Krogstad *et al.*¹² in a turbulent boundary layer with a Reynolds number approximately 3 times larger than the present one are also very close to our results, particularly those obtained with their smallest probe separation. There are, instead, significant quantitative differences with the experimental measurements by Khoo *et al.*,¹⁴ which yield $C_u^+ \approx 13$ in the whole viscous sublayer of a channel flow at $Re_\tau = 390$, and $C_u^+ \approx 15$ for boundary layers with values of the Reynolds number approximately three times higher than Krogstad *et al.*¹² It would be interesting to verify whether the difference between these two experiments can indeed be ascribed, as Khoo *et al.* suggest, to Reynolds number effects, but, although the calculation of C in a DNS at a Reynolds number $\mathcal{O}(1000)$ is presently difficult to be achieved, from the comparison of Krogstad *et al.*¹² with our results Reynolds-number effects seem very mild.

VI. TAYLOR HYPOTHESIS

As already noticed by others,^{10,11,14} the very concept of convection velocity is necessary for a correct application of the commonly used Taylor's hypothesis. It is clear that it is this velocity, and not the local mean velocity, that must be used to convert temporal data into spatial data and *vice versa* within the limits in which this is possible. The assessment of such limits by means of comparison of frequency and wavenumber-transformed spectral data, as already performed in previously published papers,^{10,11} does suffer however from the difficulties mentioned before, namely from the uncertainty related to the estimation of spectral density functions from a statistical sample of finite size.

A quantitative check of Taylor's hypothesis without such statistical uncertainties can be obtained by means of correlation functions. Figure 5 reports the autocorrelation function for the longitudinal shear at the wall: The continuous line is the plain $R(\xi^+, 0)$ correlation drawn up to half the channel length, whereas the dashed line is the $R(0, \tau^+)$ function plotted versus the abscissa $C_u^+ \tau^+$, with C_u^+ evaluated at the wall.

The agreement is generally good, and in particular is very good for values of the correlation larger than 0.5. It is, however, evident that a range of separations does exist, where the simple space-time conversion through the convection velocity is not enough for the space and time correlation functions to coincide. In order to enhance our ability to discern the quantitative differences between these two curves, they have been drawn in Fig. 5 compensating for the effects of the spurious, periodicity-induced secondary peak through an exponential fitting, and truncating at its first local minimum.

The curves start being appreciably different at a spatial separation of $\xi^+ = 150$, and an error of $\approx 15\%$ is made for a still statistically significant value of the correlation function of 0.1.

VII. DISCRETIZATION EFFECTS

Since the autocorrelation of the longitudinal component of friction is the most extended over both time and space, as seen from Figs. 1 and 2, this is the appropriate quantity to be looked at in order to verify the suitability of the longitudinal size of the computational box. The minimum correlation along the section at $\tau = 0$, which is usually considered for this purpose, occurs at a separation equal to half the channel length for symmetry reasons (see Fig. 1 again), and is 0.042 for our box size. It becomes 0.049 if the u -velocity correlation is evaluated at $y^+ = 10$ rather than at the wall. But other potential candidates must be examined, for example, the minimum correlation along a section at $\xi = 0$. More generally, since the correlation function is made artificially periodic along the ξ axis by the periodic boundary conditions, and can be seen as the superposition of repeated images of the true correlation function, a good measure of the separation between such images is given by the maximum along the line of minima that separates two successive correlation peaks. The temporal autocorrelation of the longitudinal shear stress at zero spatial separation has been already shown in Fig. 3 (dashed line): Its first minimum is 0.028 (0.04 for the u component at $y^+ = 10$).

The comparison between the two autocorrelation minima along the section at $\tau^+ = 0$ and along the section at $\xi^+ = 0$ indicates that the former provides a slightly more stringent constraint on the size of the computational box. In fact, an analysis of the full ξ, τ plane shows that, at least for the present box length ($L_x = 4\pi h$), the largest of all autocorrelation minima in the gap between two repeated images of the correlation surface occurs at $\xi = L_x/2$ and $\tau = 0$, i.e., at the classically assumed point for such tests. This remains, therefore, the most reliable choice even when the full ξ, τ -plane is taken into consideration.

On the other hand, the all-encompassing question of how small is small enough remains difficult to answer. Can we consider an autocorrelation of 0.049 negligible at all? Or, on the contrary, is it perhaps unnecessarily small (as the minimal-channel concept²¹ is sometimes implied to suggest)?

A further simulation has been performed for a longer channel with $L_x = 8\pi h$ and the number of longitudinal Fourier modes increased to 385 in order to keep the spatial reso-

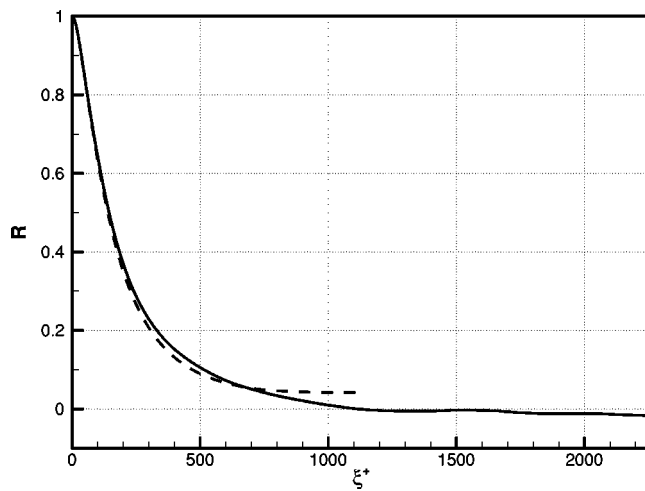


FIG. 6. Comparison between the autocorrelation function $R(\xi^+, 0)$ of the longitudinal component of wall friction, for two simulations with different channel lengths. The dashed line is obtained with a computational box of standard length $L_x = 4\pi h$, and the continuous line corresponds to a box of twice that length, i.e., $L_x = 8\pi h$.

lution unchanged. The results of this demanding computation are shown in Fig. 6 in terms of the autocorrelation function $R(\xi^+, 0)$ of the longitudinal wall friction at zero time delay, compared with the same quantity from the case with $L_x = 4\pi h$. It can be seen that the channel length used in most of the DNS research papers published to date actually determines a spurious behavior of the autocorrelation function at large separations, whereas the use of twice that length guarantees that $R(2\pi h, 0)$ can decrease to zero without unphysical constraints due to the finiteness of the computational box. The autocorrelation at the maximum streamwise separation for the longer channel reaches -0.016 , i.e., decreases down to the level where only the error implied by the finite integration interval becomes significant.

The convection velocity of flow perturbations, insofar as representing the advection of turbulent structures, is likely to be sensitive to numerically induced alterations in the key physical quantities of turbulent wall flow, and might well be taken as an indicator of box-length suitability. For this reason we investigated the effect of the main computational parameters on the calculation of \mathcal{C} .

Since our definition of convection velocity is based on the direction of maximum correlation at the smallest time delay represented in the calculation, we first checked the effect of the choice of the time-step Δt . Repeating a simulation with $\Delta t^+ = 0.15$, i.e., twice the normal value, has not given any discernible difference.

We then moved on to the effect of the finite periodic box. To test its importance, besides the simulation with the longer channel we performed an additional simulation on a box with $L_x = \frac{4}{3}\pi h$ and $L_z = \frac{2}{3}\pi h$, leaving the spatial resolution identical to the previous case and hence using 65 Fourier modes in either direction. Results from the standard and the longer channel length simulation are very similar, with small differences being probably attributable to the finiteness of the sampling interval. On the other hand results in terms of the computed convection velocity are shown in Fig. 7 for the small-

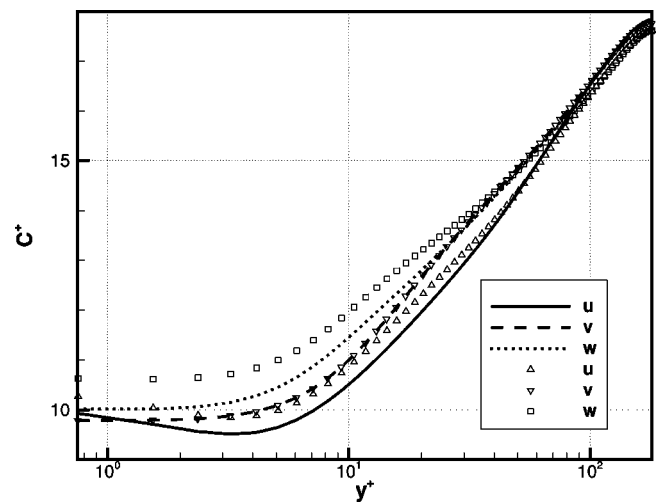


FIG. 7. Effect of the box size on convection velocity: Comparison between profiles for the large channel with $L_x = 4\pi h$, $L_z = \frac{4}{3}\pi h$ (lines) and for the small channel with $L_x = \frac{4}{3}\pi h$, $L_z = \frac{2}{3}\pi h$ (symbols).

and standard-size channels, and indicate for the three velocity components a clear dependence of \mathcal{C} on box size.

The size of the latter channel is such that the wall area considered is still several times bigger than the minimal flow unit described by Jiménez and Moin,²¹ and in particular the length of the computational box is more than twice as much. Minimal channel simulations reportedly allow a reasonable computation of low-order turbulence statistics, especially in the near-wall region, and only exhibit some differences with full-channel simulations in the outer region of the channel. Our definition of convection velocity focuses on the smallest spatio-temporal scales resolved by the simulation, so that an effect of the box size might not on this basis be expected, especially in the near-wall region. Such an effect is nevertheless clearly appreciable and significant: It turns out that in a medium-sized channel the propagation velocity of the fluctuations in the near-wall region is overestimated by 5%–7%, with the error slowly decreasing farther away from the wall but still appreciable at $y^+ \sim 80$. This means that results from narrow-channel simulations must be considered with care, since they might be comparable with results from a simulation with adequate box size insofar as *some* low-order turbulence statistics are concerned, but other important physical properties of the flow are misrepresented.

VIII. CONCLUSIONS

Space-time autocorrelation data naturally allow a distinction between the concept of time of transit of a flow structure at a given spatial position (directly related to its length), and the temporal extension over which the structure can be followed in its motion (i.e., its life time). We propose an integral time scale T^ℓ to be adopted for the characterization of structure life time in turbulent wall flows. Unlike the standard integral time scale, computed from time correlations at zero space separation (or from space correlations at zero time separation, the approximate conversion between

the two being possible according to Taylor's hypothesis), this life scale is the integral of the space-time correlation function along the line of its spatial maxima in the ξ, τ plane. Instead of adopting a fixed-in-space view (typical of fixed-point experimental measurements) or a fixed-in-time view (very natural to numerical analysts, who can take snapshots of the full computed flow field), this time scale relies on the statistical observation of the flow in a pseudo-Lagrangian frame that moves so as to maximize the space-time correlation. (A similar approach has also been recently pursued from an experimental standpoint,²² at least for homogeneous isotropic flows, by following flow particles along their trajectories.) This new time scale quantifies the different life span of the fluctuations of different near-wall flow variables. It brings out, for example, that pressure fluctuations, characterized by much shorter space and time scales than the u velocity, are just half as long-lived.

The convection velocity of turbulent fluctuations is a concept which naturally arises from the previous analysis. The convective nature of the flow is evident from the elongated shape of the autocorrelation contours, even at the wall where the local mean velocity is zero. The correlation at the wall propagates downstream at a speed dictated by the outer structures running past; this speed is higher for pressure fluctuations, and lower for the velocity components. We propose to define and compute the convection velocity from correlation data instead of spectral data, since the statistical error in the former case is confined to the largest separations, whereas in the latter it is uniformly distributed over the entire wavenumber and frequency range, and does not decrease with an increase in sample size. (This error might be diminished by averaging over the whole spectrum, which eventually amounts to the same operation as Fourier-transforming back to the correlation function.) For definiteness we evaluate \mathcal{C} from the direction in the ξ, τ plane where the space-time correlation attains its maximum at the origin, or in practice at one numerical time step of the simulation. Our results reconfirm previous numerical evaluations of \mathcal{C} but only some of the available experimental data, in which a non-negligible scatter is present. A doubt remains whether this scatter can indeed be attributed to Reynolds-number effects, or perhaps is due to limitations in the experimental techniques.

A quantitative verification of Taylor's frozen-turbulence hypothesis has been made in terms of correlation functions. Of course Taylor's hypothesis is only an approximation, and if the convection velocity is computed based on information for the smallest scales, then some discrepancy is unavoidable in the medium-scales range. The quantification of this effect is rather difficult in terms of spectral data, whereas it becomes relatively easy in terms of correlation functions: A 15% error is reported in a wide range of separations where the correlations functions are still statistically significant.

Finally, spatio-temporal autocorrelation functions for wall shear, wall pressure and velocity fluctuations have been used for a critical discussion of the effect of discretization parameters on the current procedures for the direct numerical simulation of wall turbulent flows with periodic boundary conditions. Starting from an overall consideration of the full spatio-temporal correlation in the choice of a suitable

streamwise length of the computational domain, we find that the classical criterion based on spatial correlations remains the most stringent, at least for the parameters considered in the present study. Based on this criterion, results from a demanding simulation where the channel length has been doubled while keeping the spatial resolution unchanged has shown that a channel length of $L_x = 8\pi h$ could be necessary, at the present values of the other computational parameters, for the correlations at the maximum streamwise separation to decrease to a level where the error implied by the finite integration interval becomes predominant.

In the same context, we also checked the sensitivity of the computed value of \mathcal{C} to the parameters of the numerical discretization. In particular we found a negligible effect of the time step size, but a significant effect of the size of the computational periodic box. Despite our definition of convection velocity only involves the correlation at infinitesimal time and space separation, a reduced computational box determines an overestimation of the convection velocity, for all the velocity components, of the order of 5%–7%. The fact that this inadequate computational box is still more than twice as long as the minimal channel unit, i.e., the minimal box required for wall turbulence to be self-sustained, is a clear indication that verifying the results of a few low-order statistics is not enough to establish the suitability of a given direct numerical simulation of turbulence. Perhaps the convection velocity might be proposed as an indicator for this purpose.

¹A. Johansson, P. H. Alfredsson, and J. Kim, "Evolution and dynamics of shear-layer structures in near-wall turbulence," *J. Fluid Mech.* **224**, 579 (1991).

²J. Kim and F. Hussain, "Propagation velocity of perturbations in turbulent channel flow," *Phys. Fluids A* **5**, 695 (1993).

³G. I. Taylor, "The spectrum of turbulence," *Proc. R. Soc. London, Ser. A* **164**, 476 (1938).

⁴A. J. Favre, J. J. Gaviglio, and R. J. Dumas, "Space-time double correlations and spectra in a turbulent boundary layer," *J. Fluid Mech.* **2**, 313 (1957).

⁵A. J. Favre, J. J. Gaviglio, and R. J. Dumas, "Further space-time correlations of velocity in a turbulent boundary layer," *J. Fluid Mech.* **3**, 344 (1958).

⁶W. R. B. Morrison, K. J. Bullock, and R. E. Kronauer, "Experimental evidence of waves in the sublayer," *J. Fluid Mech.* **47**, 639 (1971).

⁷H.-P. Kreplin and E. Eckelmann, "Propagation of perturbations in the viscous sublayer and adjacent wall region," *J. Fluid Mech.* **95**, 305 (1979).

⁸J. Kim, P. Moin, and R. Moser, "Turbulence statistics in fully developed channel flow at low Reynolds number," *J. Fluid Mech.* **177**, 133 (1987).

⁹U. Piomelli, J.-L. Balint, and J. M. Wallace, "On the validity of Taylor's hypothesis for wall-bounded flows," *Phys. Fluids A* **1**, 609 (1989).

¹⁰H. Choi and P. Moin, "On the space-time characteristics of wall-pressure fluctuations," *Phys. Fluids A* **2**, 1450 (1990).

¹¹S. Jeon, H. Choi, J. Y. Yoo, and P. Moin, "Space-time characteristics of wall shear-stress fluctuations in a low-Reynolds-number channel flow," *Phys. Fluids* **11**, 3084 (1999).

¹²P.-A. Krogstad, J. H. Kaspersen, and S. Rimestad, "Convection velocities in a turbulent boundary layer," *Phys. Fluids* **10**, 949 (1998).

¹³B. C. Khoo, Y. T. Chew, and C. J. Teo, "On near-wall hot-wire measurements," *Exp. Fluids* **29**, 448 (2000).

¹⁴B. C. Khoo, Y. T. Chew, and C. J. Teo, "Near wall hot-wire measurements. Part II: turbulence time scale, convective velocity and spectra in the viscous sublayer," *Exp. Fluids* **31**, 494 (2001).

¹⁵W. R. C. Phillips, "Eulerian space-time correlations in turbulent shear flows," *Phys. Fluids* **12**, 2056 (2000).

¹⁶M. Quadrio and P. Luchini, "A 4th order accurate, parallel numerical method for the direct simulation of turbulence in cartesian and cylindrical

- geometries," in Proceedings of the XV AIMETA Conference on Theoretical and Applied Mechanics, 2001.
- ¹⁷R. Moser, J. Kim, and N. N. Mansour, "Direct numerical simulation of turbulent channel flow up to $Re_\theta=590$," *Phys. Fluids* **11**, 943 (1999).
- ¹⁸H. Wang and W. K. George, "The integral scale in homogeneous isotropic turbulence," *J. Fluid Mech.* **459**, 429 (2002).
- ¹⁹G.-W. He, R. Rubinstein, and L.-P. Wang, "Effects of subgrid-scale modeling on time correlations in large eddy simulations," *Phys. Fluids* **14**, 2186 (2002).
- ²⁰J. S. Bendat and A. G. Piersol, *Engineering Applications of Correlation and Spectral Analysis* (Wiley, New York, 1980).
- ²¹J. Jiménez and P. Moin, "The minimal flow unit in near-wall turbulence," *J. Fluid Mech.* **225**, 213 (1991).
- ²²N. Mordant, J. Delour, E. Lévêque, A. Arnéodo, and J.-F. Pinton, "Long time correlations in Lagrangian dynamics," in *Advances in Turbulence IX*, edited by I. P. Castro, P. E. Hancock, and T. G. Thomas, Proceedings of the IX European Turbulence Conference, 2002, pp. 732–735.